Is dust an important source of aerosol particles in northern Europe?

Author: Hiroki Nagatomi

Bachelor thesis, Lund University, March 12, 2024

Supervisors: Adam Kristensson, Göran Frank, Lund University, Division of Combustion Physics.

LUNDS UNIVERSITET

Abstract

Aerosols are one of the significant factors influencing climate, environment, and human health. They are categorized into anthropogenic and natural sources. In Sweden, natural aerosol sources of high coarse mode particle mass concentrations for particles larger than 1 μm in diameter include sea spray, primary biogenic particles, and dust particles. The dust particles can be agricultural soil and mineral dust, road dust, high-latitude dust, and transport of dust from the Saharan Desert. These sources exhibit local, regional, or even long-distance transport characteristics. Classifying these natural aerosol sources is beneficial considering their impacts.

This study aimed to identify transport events of coarse particles from the Saharan Desert, and estimate source contribution of coarse mode dust particle mass concentration in Hyltemossa, southern Sweden (56.098N 13.419E). Observational data of PM_{10} and PM_1, meteorological data, and ceilometer backscatter data were used during spring seasons between 2018 and 2023. The analysis focused on extracting periods of high concentrations considered as dust events using 24-hour average mass concentration of PM_{10-1}, and further examining four periods (each a week duration) with high afternoon peak concentrations based on hourly averages.

One occasion with dust transport from Sahara was identified using the ceilometer data, with transport via France, the UK, and Norway between March 20 and 23, 2020. The ceilometer analysis proved difficult to perform, why it needs supplement from other complementary remote sensing analysis.

The results suggested that the afternoon dust peak events during the selected four periods were likely caused by dust blowing up from near-regional road and agricultural areas, facilitated by the formation of the convective boundary layer and increasing wind speeds from daytime to afternoon. Contribution rates to total mass concentration from dust ranged from 10% to 22% for the four periods, with an estimated mass concentration of PM_{10-1} between 1 and 2 μg/m^3. This was considered as a minimum estimate of dust contribution.

Table of Contents

1. Introduction

1.1 Background

Observation of aerosols in the atmosphere is crucial for considering climate, environment, and human health impacts. Currently, many countries and regions have regulations regarding emissions from transportation, and various policies are implemented to improve air quality.

Atmospheric aerosols can be classified into those of anthropogenic and natural origins. Once released into the atmosphere, distinguishing between them becomes challenging. Major anthropogenic emission sources in Sweden include industrial and transportation emissions, emissions from ships, wood burning for heating in winter, transportation from neighboring countries, dust from paved roads, asphalt particles from studded tires in spring, while natural emission sources include sea salt particles, primary biogenic aerosol particles, and dust particles (Sabelström et al., 2023). Different dust aerosols can be agricultural soil and mineral dust, road dust, high-latitude dust, and long-distance transport of dust from the Saharan Desert. These natural emission sources can come from varying distances from the measurement location, and can therefore be of local, near-regional, and long-distance nature. The geographical distribution of their concentrations is known to decrease towards the northern parts of Sweden, attributed to the proximity of the southern regions to large continental emission sources and high population density (Malin Gustafsson et al., 2018).

Dust transport events from deserts are also sometimes observed in East Asia. Dry regions such as the Taklamakan Desert, the Gobi Desert, and the Loess Plateau in China bring yellow sand to China, Korea, and Japan. While the impact of yellow sand is a common issue in the East Asian region, even in relatively distant Japan, flight cancellations and disruptions in transportation networks can occur. Currently, observations of yellow sand are conducted at 11 monitoring sites in Japan, including Tokyo, Osaka, Nagoya, and Fukuoka.

Kristensson and colleagues have previously discovered that half of the PM_{10} mass concentration in rural areas of southern Sweden during spring is attributed to dust aerosols (PM10 refers to particles with a diameter of less than 10 μm) (Kristensson et al., 2005). Such particles in the micrometer range have adverse health effects through inhalation in the human respiratory system and scatter or absorb shortwave radiation and influence the formation process of ice nuclei, highlighting the significance of understanding the sources of these dust particles in climate science.

Research in Stockholm suggests that approximately 30 deaths per year are estimated to be caused by micrometer-sized particles mainly from roads (Meister et al., 2012, Environ. Health Persp., 120, 431-436), why these are important from a health-point of view.

1.2 Objectives

This study aims to identify periods with high 24-hour averaged aerosol mass concentrations of coarse mode particles during spring periods at the Hyltemossa field site in southern Sweden between 2018 and 2023. In addition, occasions with occurrence of high hour-averaged mass concentrations in the afternoon, likely caused by dust emissions were also investigated, and it was quantified how much they contributed to coarse model particle mass concentrations.

Whether these two types of high concentration episodes originated from Saharan dust episodes or from other types of dust sources was further investigated.

2. Method

2.1 Measurement location description and measurement period

The Hyltemossa field site (56.098N 13.419E) is located in the Scania region of southern Sweden (Figure 1). Hyltemossa is about 60 km northeast of Malmö, Sweden's third largest city, and is surrounded by the sea on the east, west, and south sides on the order of 50 km away from Hyltemossa. Therefore, although the area surrounding the observatory is forested, sea salt particles are frequently measured at the site depending on the wind direction and wind speed. In addition, the proximity to continental areas to the south, makes it a relatively polluted environment during southerly wind directions.

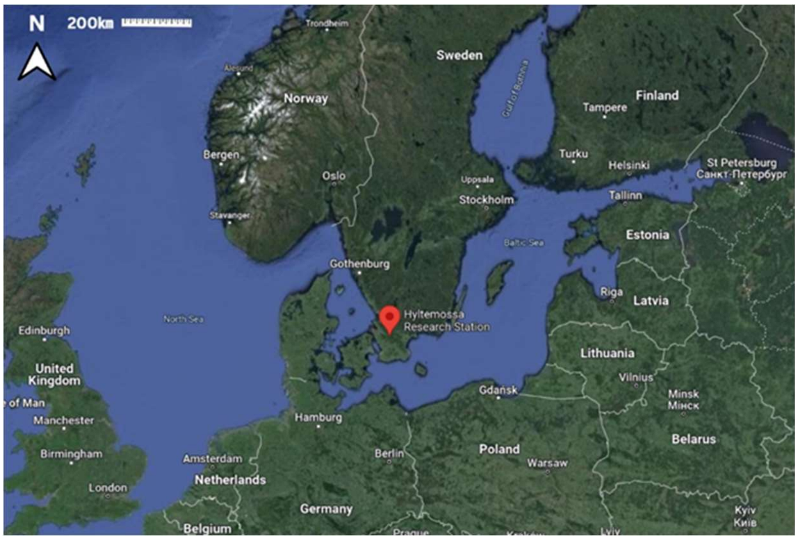

Figure 1: *Satellite image of Hyltemossa Research Station in Southern Sweden (Google-Maps, 2024).*

Hyltemossa is home to one of the Integrated Carbon Observation System (ICOS) infrastructure stations. ICOS is a European network of more than 170 stations in 16 European countries that conduct atmospheric, ecosystem, and oceanographic observations. Hyltemossa station provides atmospheric and ecosystem observations and has a 150-meter main mast for atmospheric observations. At different altitudes, meteorological data and gas concentrations are measured.

Hyltemossa also belongs to the Aerosol, Clouds and Trace Gases Research Infrastructure (ACTRIS) dedicated to the research about clouds, aerosol particles and their gaseous precursors. ACTRIS hosts 113 stations all around Europe and the rest of the world. Hyltemossa is one of the 79 aerosol in-situ stations measuring aerosol particles at ground level.

Up until December 2022, the PALAS FIDAS particle measurements took place at a third location, namely the Hallahus field site (56.02327N, 13.08544E), situated approximately 19 km to the west of the Hyltemossa field site (Figure 2). It belongs to the Swedish Environmental monitoring program of air pollutants.

The surrounding area around the 150 m ICOS mast is dominated by *Picea abies* (Norway spruce), *Betula sp.* (birch), and *Pinus sylvestris* (Scots pine). The forest belongs to the temperate region. The closest anthropogenic influence is a two-lane road 500 m to the west. About 5 km to the north-northwest is the village of Perstorp, which has a population of about 6,000. There are also close by houses a few hundred meters away to the north-west, where it is possible that people heat up their homes with domestic wood combustion.

Figure 2: *Satellite image showing the location of Hallahus measuring station, Hyltemossa Research station and ACTRIS station (Google-Maps, 2024).*

The ACTRIS measurements take part about 600 m north of the ICOS 150 m mast observation facility. The ACTRIS station building is surrounded by a small cow pasture, and otherwise by mixed deciduous and coniferous forests at further distances, for example the Scots Pine forest a few hundred meters to the south surrounding the 150 m ICOS mast.

The Hallahus station facility is surrounded by a small grassland area, with mixed deciduous and coniferous forests around the grassland. There are two small cottage houses about 200 m away to the southwest and south from the station house. A main road passes along a west-to-east transect about 400 m to the south of the station.

The instruments at Hyltemossa and Hallahus are operating continuously, but data for this thesis were collected from years 2018 until 2023, during spring periods March to May. This was based on the likely occurrence of dust events in spring, when the soil is drier in southern Sweden and agricultural fields are bare before crops have started to grow on the fields, increasing the likelihood of wind-blown soil dust.

2.2 Instrumentation

2.2.1 PALAS-FIDAS instrument

The Palas-FIDAS instrument is a device for measuring the mass concentration of fine particulate matter (PM) in the atmosphere. It was used in this study to measure the concentration of coarse mode particles between 1 and 10 μm in diameter (PM_{10} minus PM_1). Its principle of operation is optical particle measurement using light scattering. A sample is taken from an inlet, the particles are passed through a laser, and the laser scatters them. The amount and angle of light scattering depends on the size of the particles; larger particles scatter more light. The particle size distribution can then be determined from the data obtained from the detector. (FIDAS manual (2021))

The FIDAS instrument was located at Hallahus environmental monitoring field site between 2018 and 2022, and then it was moved to the Hyltemossa ACTRIS field site at the start of 2023.

2.2.2 ICOS measurement tower in Hyltemossa

Meteorological data used from the 150 m ICOS mast were hourly averaged temperature (℃), relative humidity (%), and wind speed (m/s). Soil moisture content at various depths around the mast and solar radiation intensity at an altitude of 50 m were also used in the analysis to study periods when the soil was dry and when winds could potentially stir up windblown dust due to turbulent convection initiated by intense solar radiation. These data represent a sub-sample of all available meteorological data and greenhouse gas sampling at the 150m mast. (Figure 3)(ICOS/National Network Sweden)

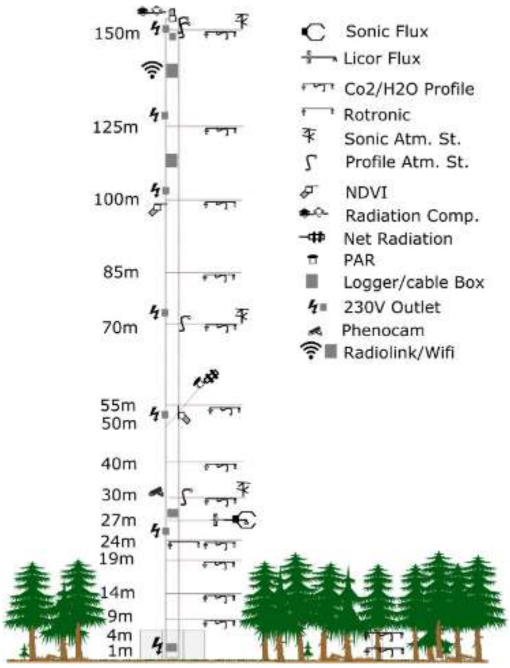

Figure3. *Scheme of all measurements at the tall tower in Hyltemossa (ICOS/National Network Sweden)*

2.2.3 Ceilometer data

EUMET Net e-profile (E-PROFILE) is part of the EUMETNET Composite Observing System (EUCOS), which manages a European network of ceilometers, radars and automatic lidars for monitoring the vertical distribution of aerosols, and clouds. The network of ceilometers in Europe was used in this study to observe Saharan dust transport in different vertical layers from southern Europe to Sweden.

A ceilometer is a device that uses a photodetector to measure the backscatter from vertical obstacles in the atmosphere. the LIDAR technique allows the acquisition of various atmospheric parameters such as cloud base height, boundary layer height, and visibility. once every 16 seconds, a 910 ㎚ diode laser pulse is transmitted vertically. The backscatter from cloud particles, aerosol particles, and other atmospheric obstacles is then detected with a resolution of 10 m and analyzed by the instrument to produce vertical backscatter profiles of up to 15 km and calculate the height and BLH of the three cloud layers. (Carneheim,E.(2020))

2.3 Modeling

Daily Dust Products of Saharan dust transport to Europe provided by the WMO Barcelona Dust Regional Center were used to study dust transport from Sahara to Sweden. The WMO Barcelona Dust Regional Center publishes a wide variety of modeling systems, and for this analysis, MULTI-MODEL published by AEMET (Basart et al., 2019) and MONARCH (Pérez et al., 2011) (Ninkovic, S et al., 2016) published by the BSC were used to simulate aerosol optical depth (AOD) and Load respectively.

3. Analysis Method

3.1 Selection of analysis periods by 24-hour averages

In this study, the PM_{10} and PM_1 mass concentration [μg/m^3] data from the PALAS-FIDAS instrument was used. The period covered was a total of 491 days in the spring season from March to May during the years 2018 to 2023. PM_{10-1} was selected as the variable of interest to study coarse mode particles (1-10 μm diameter).

Periods when 24-hour averages of PM_{10-1}-concentrations were higher than 7 μg/m^3, where searched for. It is expected that a major fraction of coarse mode particle mass concentrations is stemming from dust events when the PM_{10-1}-concentrations was higher than 7 μg/m^3. The periods found are tabulated in section 4.1.

Certainly, also periods with lower PM_{10-1}-concentrations should be containing a fraction of dust particles and a part of periods with PM_{10-1}-concentrations higher than 7 μg/m^3 were not stemming from dust events. However, this was a first screening of the data set of dust events. When someone takes over the work after this study, that person can look further for dust events during other periods, using for example source apportionment techniques to attribute PM_{10-1}-concentrations to dust particles.

3.2 Afternoon peaks and meteorological data

The one-hour averages for the same period of days from the previous section 3.1 (days with a 24-hour average PM_{10-1} mass concentration of 7μg/m^3 or higher) were further investigated for the occurrence of dust particles in afternoons. Namely, it has been detected that there were afternoon peaks in PM_{10-1}-concentrations that lasted for several hours, that were likely originating from dusting events.

The characteristics of such days with afternoon peaks was that the height of the boundary layer hight (BLH) increased from a nocturnal type shallow boundary layer into a convective type boundary layer at lunch-time and in the afternoon. The increase in BLH was simultaneous with a rise in global radiation, atmospheric temperature, and wind speeds during daytime, while the decrease of BLH was associated with reduced wind speeds during the nighttime during conditions with clear skies. Also, soil moisture decreased over an extended period. Therefore, this was interpreted as an uplift of dusting from the soil and road surfaces nearby due to the convective turbulence in midday and afternoons with a concurrent drying out of the soil and road surfaces.

It should be noted that simultaneous to the PM_{10-1}-concentrations increase in the afternoons, the PM1 concentrations decreased, which indicated that the increase in BLH dispersed the anthropogenic pollutants and natural aerosol particles below 1 µm in diameter, while the PM_{10-1}-concentration increased due to increased wind-blown dust. The PM1 concentration increased during night-time due to trapping of pollutants in the shallow nocturnal boundary layer. Hence, PM_{10-1} and PM1 concentrations were anti-correlated during these periods. However, it should be noted that there could be other plausible reasons for afternoon peaks than dust.

Consequently, a search was done for all these possible afternoon peak days from the data set of 491 days with concentrations higher than 7µg/m^3 to search for this plausible dust source. The identified days have been tabulated in section 4.2. ICOS meteorological data (temperature, humidity, wind direction, wind speed, solar radiation, and soil moisture content) were thoroughly studied for these plausible days to confer the meteorological influence of these dusting events.

3.3 Calculation of Contribution Ratio during afternoon peak days

The contribution of PM_{10-1} afternoon peaks identified from section 3.2. analysis to the total PM_{10-1} concentration is discussed in section 4.3. and calculated according to the following equation:

$$Contribution[\%] = \frac{\sum_{k=1}^{n}\{(Peak_{ave,k} - Background_{ave,k}) * T_{peak}\}}{ALL_{ave} * T_{all}} \times 100$$

k: The number of Peak

$Peak_{ave}$: Average of PM_{10-1} mass concentration in peak time [µg/m^3]

$Background_{ave}$: Average of PM_{10-1} mass concentration in not peak time [µg/m^3]

T_{peak}: Peak hour[h]

ALL_{ave}: Average of PM_{10-1} mass concentration in the period [µg/m^3]

T_{all} ; Hour of the period [h]

Now follows an explanation how this is done in practice. We determined the difference between the average value of the afternoon peak (the red line in the figure) and the average value for the background concentration (the blue line in the figure). Then, we multiplied with the duration of the afternoon peak and divided by the average concentration during the entire period and the total duration of the period (which was more or less one week long) to calculate the contribution rate. Peak events were determined based on the steep increase and decrease rates of concentration per unit time a few hours before and after the maximum concentration during the peak event. Additionally, the definition of the background involved evenly categorizing the time periods which excluded the peak events.

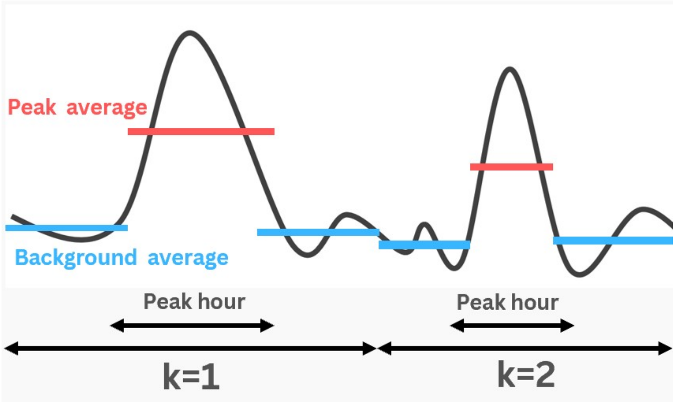

Figure3.1 *The outline diagram for calculating the contribution rate.*

This dust contribution should be regarded as a lower contribution estimate to these identified days, since dust could also contribute to the particle mass concentration outside the afternoon peak values. Nevertheless, it provides a valid estimate of how important wind-blown afternoon dust could potentially be.

3.4 Identification of events by model and ceilometer

After selecting periods when PM_{10-1} was above 7μg/m^3 in Hyltemossa, it was further investigated whether these events were due to dust from the Sahara. To investigate this, the MULTI model for AOD and MONARCH model for Load were used to identify if there was transport of dust from Sahara to Hyltemossa. An identified period of dust corresponds to an AOD value higher than 0.1 at Hyltemossa, or a Load value higher than 0.1g/m^2 at Hyltemossa. The duration and periods are tabulated in section 4.4.

Since these dust models are uncertain, it was investigated whether it was possible to validate the dust events in southern Sweden with remote sensing data. The periods obtained from the model results were consequently validated using ceilometer data. The method used an extensive network of ceilometer stations in Europe to see if transports similar to those in the model could be observed. Because the ceilometers show back scattering data as a function of height and time, it is in theory possible to quantify dust transport in different vertical layers and study how this dust is transported from one ceilometer station to another.

For example, if the dust model predicts dust were transported from the Sahara to France, Germany, and finally to Sweden, it meant that the same transport was investigated in the ceilometer data as happening in certain vertical layers. If the analysis of the ceilometer confirms dust transport to Sweden, it can be treated as a dust event that has been verified with real observable data. These results are presented in section 4.4.

4.Result

4.1 Analysis by 24-hour averages

Between 2018 and 2021, there were 491 measurement days, but only 397 days when it was possible to calculate a 24-hour mass concentration of PM_{10-1}. The number of valid days for which the 24-hour average data.

There were in total 86 days (22 %) when the 24-hour average mass concentration of PM_{10-1} was greater than 7μg/㎥ during this period (Table 4.1). Hence, there was a quite substantial number of days when the coarse mode particle concentration was relatively high, which can have impact on people exposure and health effects. These days were studied further to investigate the role of dust in these episodes.

The average mass concentration over the 397 valid measurement days was 5.27 μg/㎥ for PM_1, and 5.63 μg/㎥ for PM_{10-1}.

Table 4.1 *24-hour average values of PM_{10-1} in spring 2018-2023*

	ALL	2018	2019	2020	2021	2022	2023
Number of valid days	397	22	89	90	28	82	86
Number of days(>7μg/㎥)	86	17	23	13	2	8	23
Average[μg/㎥]	5.67	10.4	6.58	5.06	3.84	4.73	5.66
Maximum [μg/㎥]	26.2 (2019/4/23)	16.7 (2018/5/14)	26.2 (2019/4/23)	9.98 (2020/4/8)	7.83 (2021/5/14)	11.5 (2022/4/10)	13.4 (2023/5/14)

※Number of valid days are the number of days excluding with no 24-hour data from 491days

4.2 Afternoon peaks and investigation of meteorological data

The hourly average mass concentration of PM_{10-1} for the 86 days obtained from the previous section was checked, and it turned out that PM_{10-1} peaks in the afternoons were observed for 62 days of these days. As discussed in section 3.2, the PM1 concentration often anti-correlated with the afternoon peaks and midnight minimum. A subjective analysis was made on this behavior, and it was observed that this happened on 37 out of these 62 days.

To investigate these occasions in more detail, 4 periods were identified when the afternoon peaks were visible for at least 3 consecutive days. These periods were:

(i) May 13, 2018 to May 19, 2018

(ii) April 14, 2019 to April 20, 2019

(iii) March 23, 2020 to March 29, 2020

(iv) May 09, 2023 to May 15, 2023

As shown in Figures 4.1 through 4.8, the increase in concentration could be seen repeatedly during the period from about 10:00 AM to about 4:00 PM. Although it was difficult to identify the source behind the afternoon peaks, it was reasonable to hypothesize that these events were due to dust particles. Namely, Figures 4.2, 4.4, 4.6 and 4.8 showed a steady decrease of soil moisture for an extended period without rain as evidenced in the RH plots. Global radiation increased in daytime, with a subsequent increase in wind speeds at 30 m height during afternoons. This occurrence has been observed previously in other studies (Haby, 2024). However, wind speed did not increase for all days. Hence, these periods were likely to give rise to uplift of dust from the ground during dry periods with convective boundary layers in midday and afternoons.

(i) May 13, 2018 to May 19, 2018

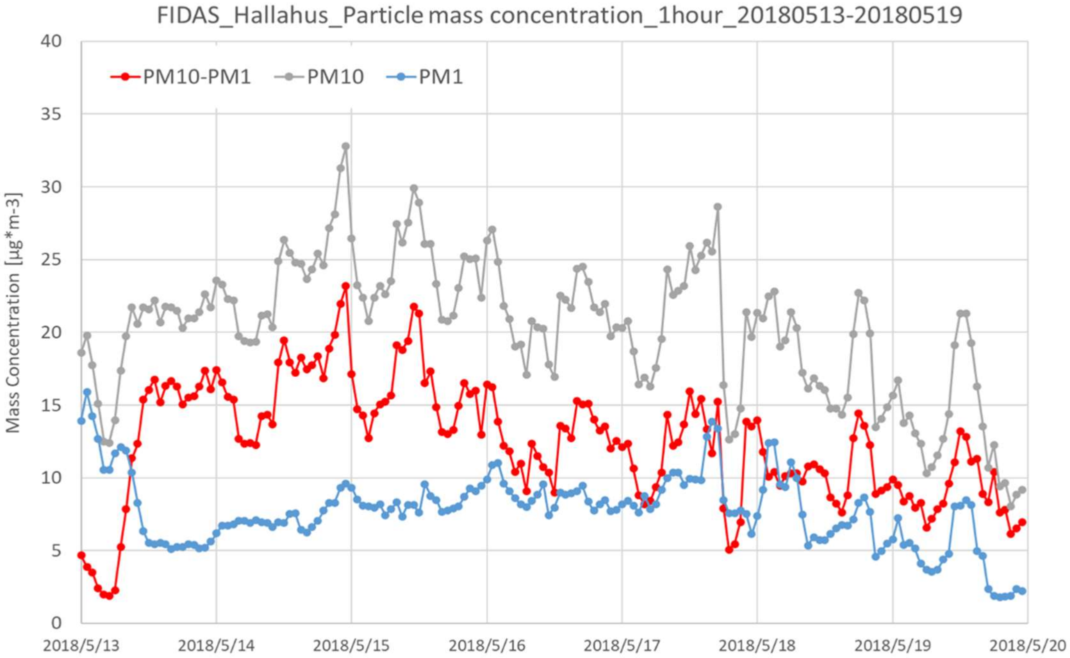

Figure 4.1 *Variation in mass concentrations of PM_{10-1}, PM_{10}, and PM_1 from May 13 to May 19, 2018 in Hallahus*

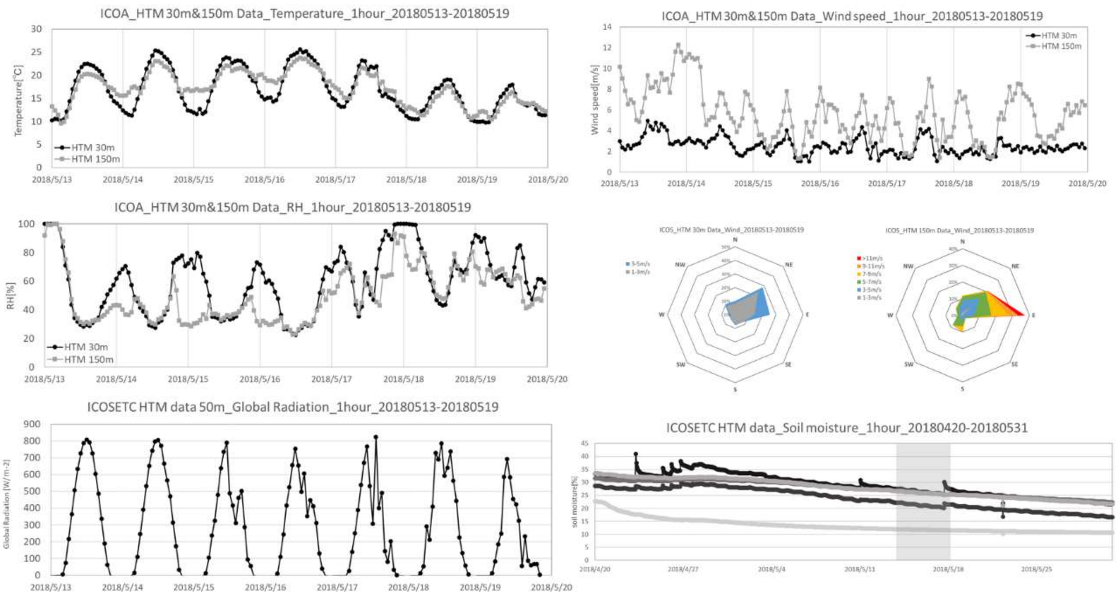

Figure 4.2 *Meteorological data for May 13 to May 19, 2018 in Hyltemossa.*

(Top left: temperature, Middle left: humidity, Bottom left: radiation intensity, Top right: wind speed, Middle right: wind direction, Bottom right: soil moisture content)

(ii) April 14, 2019 to April 20, 2019

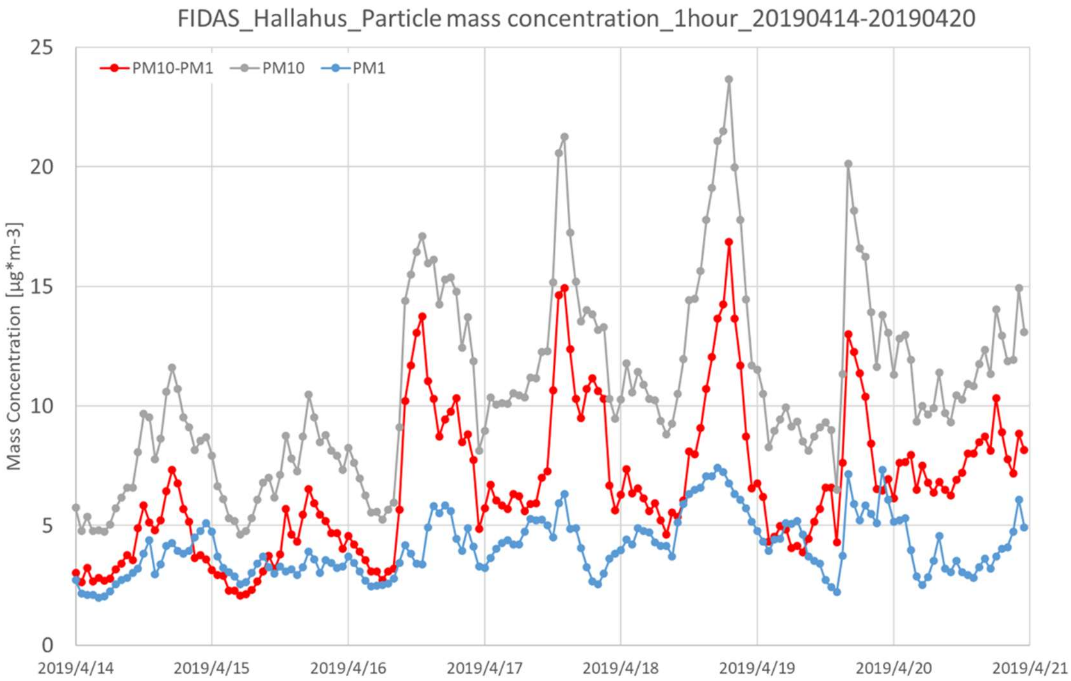

Figure 4.3 Variation in mass concentrations of PM_{10-1}, PM_{10}, and PM_1 from April 14 to April 20, 2019 in Hallahus

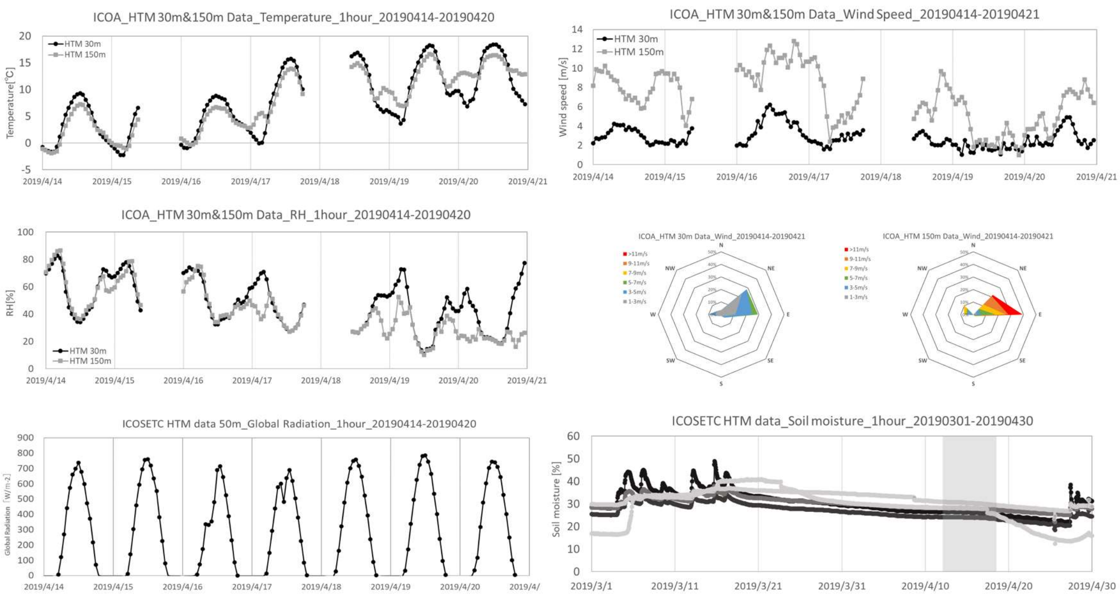

Figure 4.4 *Weather data for April 14 to April 20, 2019 in Hyltemossa*

(iii) March 23, 2020 to March 29, 2020

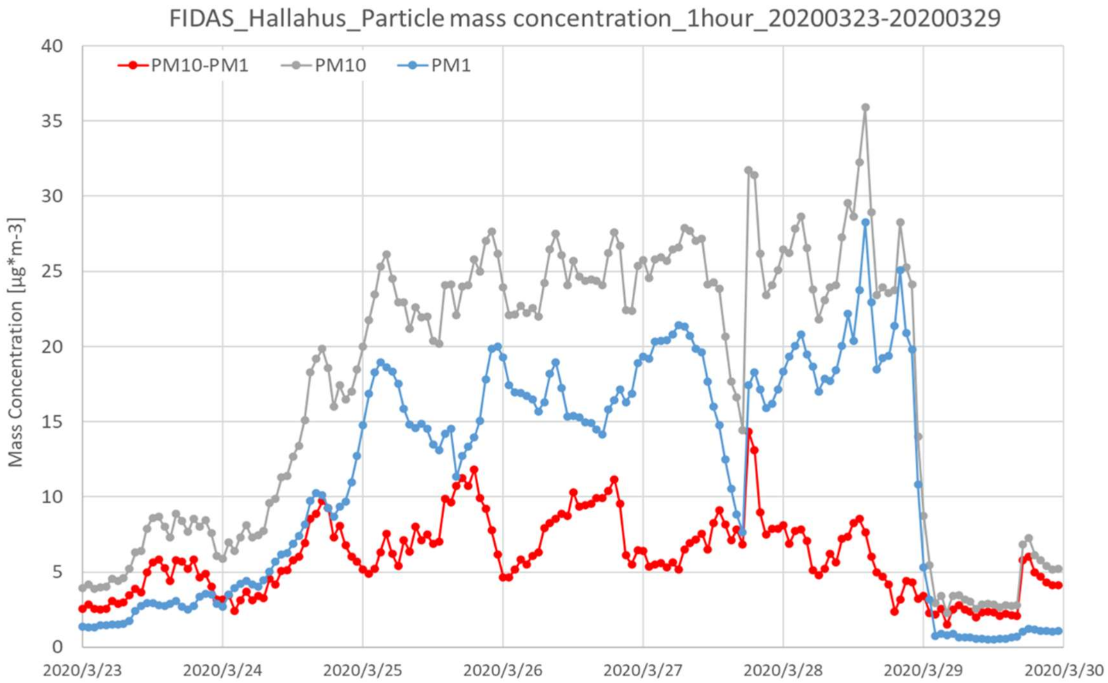

Figure 4.5 *Variation in mass concentrations of PM_{10-1}, PM_{10}, and PM_1 at Hallahus from March 23 to March 29, 2020*

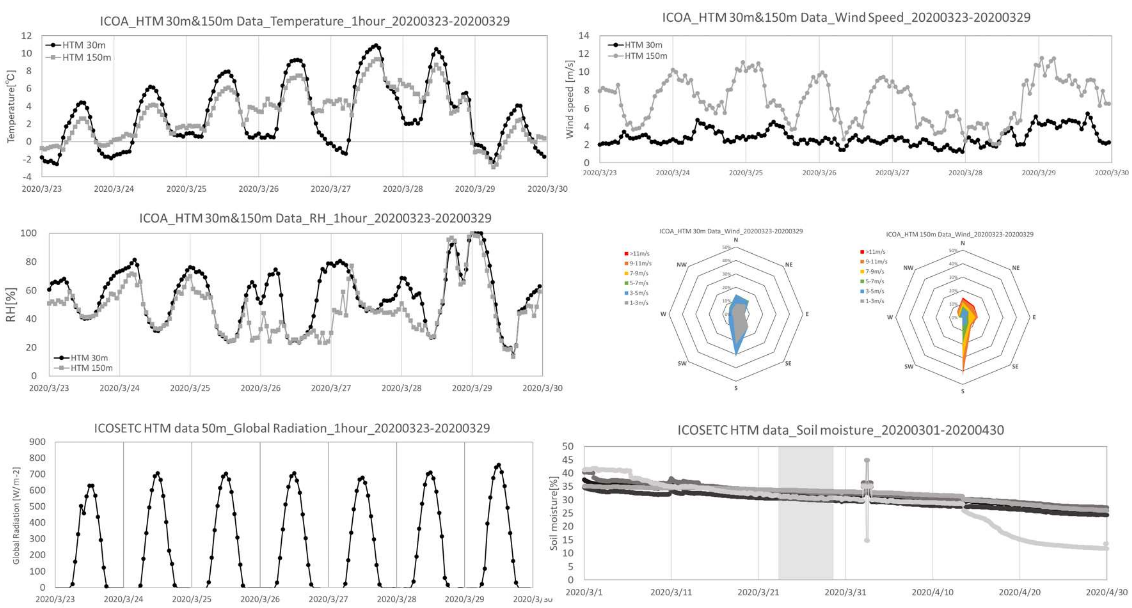

Figure 4.6 *Meteorological data for March 23 to March 29, 2020 in Hyltemossa*

(iv) From May 9, 2023 to May 15, 2023

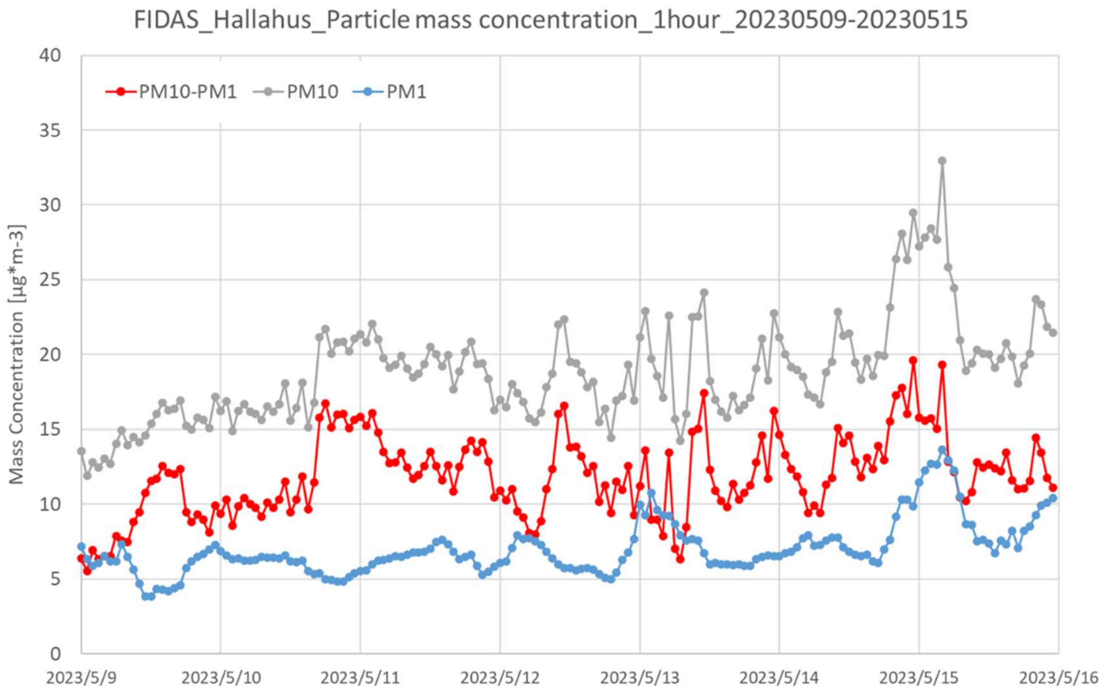

Figure 4.7 *Variation in mass concentrations of PM_{10-1}, PM_{10}, and PM_1 at Hallahus from May 9 to May 15, 2023*

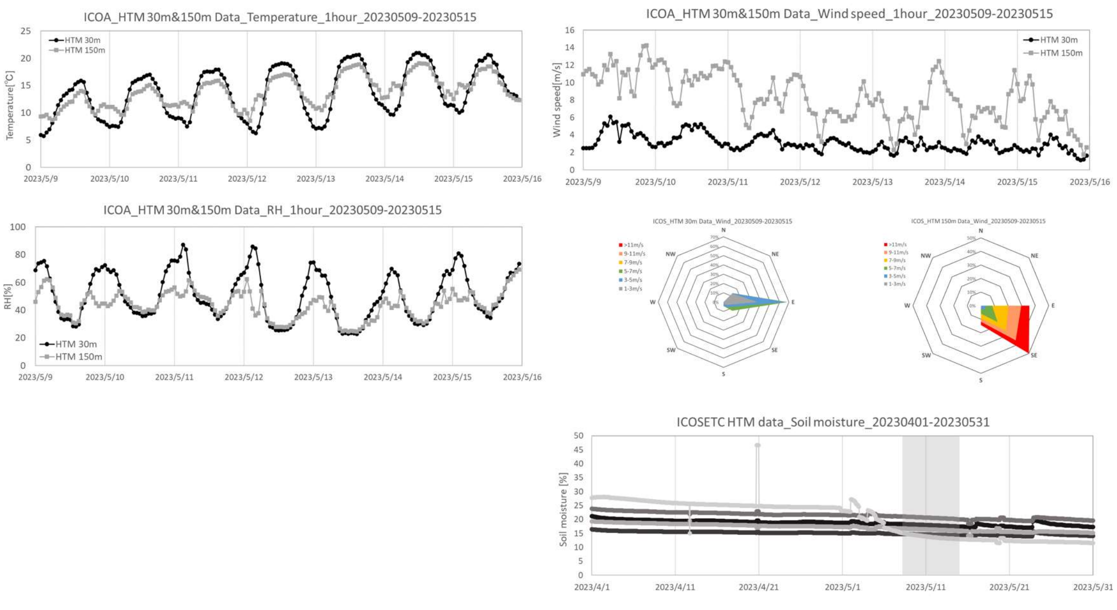

Figure 4.8 *Meteorological data for Hyltemossa from May 9 to May 15, 2023*

The wind direction was different for the different episodes, indicating that it did not really matter from where the winds originated. This again strengthens the hypothesis that it was a dust source, which should have been more dependent on other factors than where the wind came from.

4.3 PM_{10-1} Contribution Rates

As described in section 3.3, it was possible to calculate a contribution of the afternoon peaks to the PM_{10-1} average concentration during the four periods identified in section 4.2. Although there was some variation in the average mass concentrations during the periods, the contribution was confined to between 10% and 22%. The average PM_{10-1} concentrations at the time of the afternoon increase in PM_{10-1} concentrations in the afternoon were found to be between 1 and 2 µg/m^3.

Table 4.2 *Contribution of PM_{10-1} to dust (PM_{10-1}) during the afternoon peak*

Period	Number of peaks	Average[µg/㎥]	Contribution	PM10-1 mass consentration in peak[µg/㎥]
20180513-20180519	7	12.5	16.4%	2.04
20190414-20190420	7	6.66	22.0%	1.47
20200323-20200329	7	5.98	15.8%	0.956
20230509-20230518	9	11.9	10.1%	1.20

4.4 Dust model and ceilometer results

It would have been interesting to study all the periods with concentrations higher than 7 µg/m^3 from section 4.1, and if these events originated from Saharan dust events using the ceilometer method in section 3.4. However, due to diploma work constraints, only the four periods mentioned above were examined further for Saharan influence. It was plausible that the afternoon dust events identified in section 4.2 were caused by a downward mixing of air from aloft and from Sahara during midday and afternoons due to the convective boundary layer mixing. However, the dust model products of AOD and load from the 2018, 2019 and 2023 events in Table 4.2 did not show any signs of transport from Sahara, why local or near-regional dust uplift due to the convective boundary layer was a more plausible explanation for the afternoon peaks. Only during the period 2020, there were some signs of transport of dust from Sahara, and only at the beginning and the end of the 7 days period depicted in Table 4.2.

From March 20 to March 23 there seems to have been a transport of dust in the vertical layer between 2000 and 5000 m as seen in ceilometer data, roughly from France, further to Great Britan, Norway and finally southern Sweden and northern Germany. Ceilometer data indeed indicated that there was a transport on two consecutive days from France to Great Britain (Figure 4.9, March 20-21). Maybe this dust reached southern Sweden and northern

Germany as seen during the fourth day (March 23).

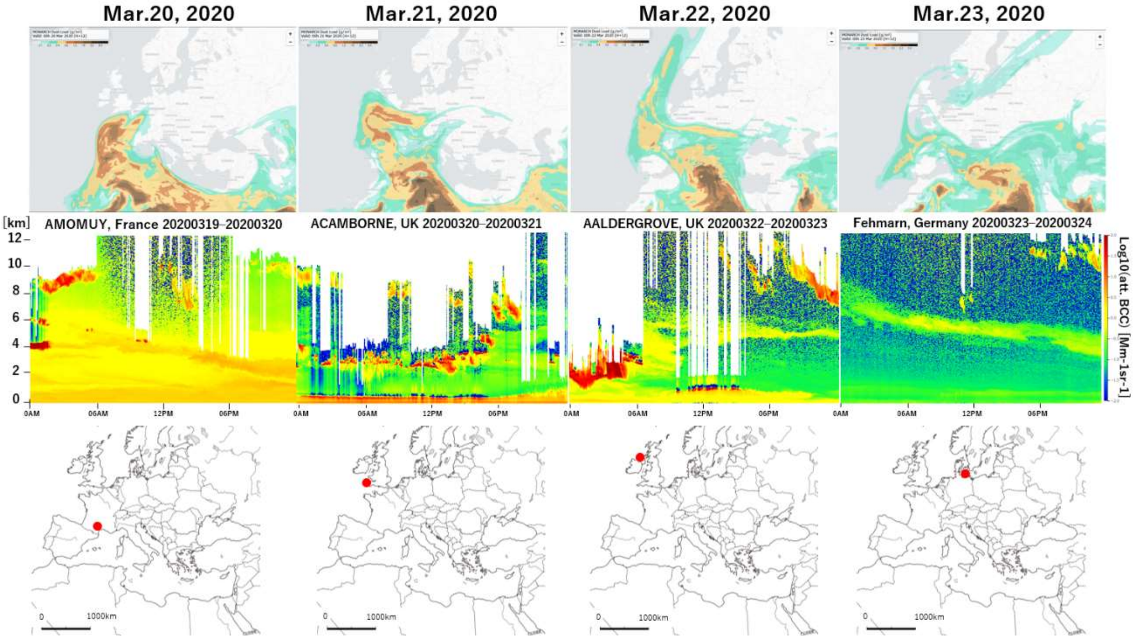

Figure 4.9 *Model results (MONARCH Load) and ceilometer results on its transport path from March 20 to March 23, 2020.*

(Top: model result (MONARCH Load), middle: ceilometer, bottom: ceilometer observation locations)

A new "tongue" of dust might have re-appeared towards March 26 and March 27 at northern Germany at a few kilometers' height (Figure 4.10). However, this still did not explain the appearance of afternoon dust peaks for the entire period March 23-29. Hence, also during this period, local or near-regional dust might have been a plausible explanation for the observed afternoon peaks.

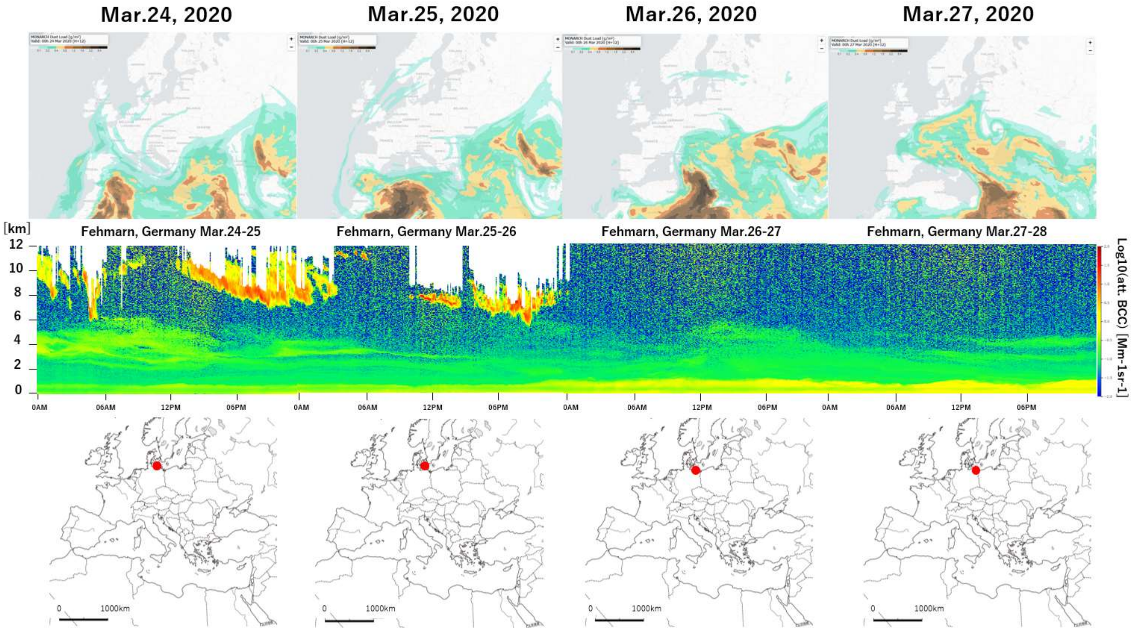

Figure 4.10 *Model results (MONARCH Load) and ceilometer results at Fehmarn, German from March 24 to March 27, 2020*

5.Discussion

5.1 Discussion of 24-hour average concentrations

In this study, 24-hour mass concentration averages of PM_{10-1} higher than 7 μg/㎥ were used in order to extract high concentration periods, that could have been dust events from the Sahara Desert. The advantage of this method was that by extracting events with relatively high mass concentrations for an extend period of 24 hours or longer, it was possible to analyze days that are more likely to be large-scale transport events.

It was not possible to prove that periods with high concentrations of PM_{10-1} were due to dust events, but the analysis here, provides the ground-work for picking up on these events, and study them further. Plausible explanations for high 24-hour concentrations in southern Scandinavia are dust events from local or near-regional dust, Saharan dust, or sea spray aerosols during high-wind speed conditions with winds from the sea, and primary biological particles.

Also 24-hour averages lower than 7 μg/㎥ could be associated with dust events, but were less clear to analyze without statistical tools such as source/receptor models. For example, there were days of modelled AOD when dust arrival to southern Sweden was forecasted, but when the 24-hour mass concentration average was below 7 μg/m^3. These identified periods were:

・March 03, 2021 to March 04, 2021
・March 30, 2021 to April 01, 2021
・April 15, 2021 to April 17, 2021
・March 16, 2022 to March 17, 2022
・April 12, 2022 to April 14, 2022

These occasions will be important to study in future for the person that picks up on this observation and investigates it further.

5.2 Discussion of afternoon peaks and meteorological data

It was speculated whether the identified afternoon dust peak events were due to convective boundary layer formation in mid-day to afternoon and increase in wind speed, blowing up dust from roads or agricultural areas. The modelled AOD and Load data indeed showed that on three of the four occasions, Saharan dust transport was not the explanation, strengthening our hypothesis of convective boundary layer uplift. The wind direction during the afternoon peak periods was different for each episode, indicating that wherefrom the wind originated was of little importance. This again strengthens the hypothesis that the dust was the source, which should depend on other factors rather than where the wind came from. In addition, sea spray aerosol are normally associated with high wind speeds from the ocean irrespective of dry soil conditions, but the analysis showed that dry soil was a prerequisite for the afternoon peak events.

However, even this circumstantial evidence is not proving it conclusively. There might be also other plausible explanations of high afternoon peaks, why this matter warrants further analysis.

5.3 PM_{10-1} Contribution rates during afternoon peaks

The mass concentration of PM_{10-1} in the peaks, as determined from the contribution rate, was approximately between 1 and 2 μg/㎥, but this value should be treated as a minimum estimate. Because this analysis covers only one week, and the background concentrations themselves could contain dust particles in part. Therefore, it is difficult to calculate an accurate contribution rate based on the contribution rate at the peak only. But this still gives an estimation of the magnitude and severity of the problem. This problem is not a major concern for health effects as discovered in this study, since it seems to occur only during dry periods in the spring, and since it contributes to a relatively low mass concentration in the afternoon peaks. However, bearing in mind future climate change and change of extended periods with dry soil conditions, might warrant a future continuation of monitoring these events.

The contribution between 1 and 2 μg/㎥ was lower than the contribution calculated by Kristensson (2005), where dust contributed to about 5.0 μg m^{-3}. However, the Kristensson study included all sources of dust using source/receptor modelling, while the current estimate only included the afternoon dust peaks.

5.4 Discussion of Dust Model and Ceilometer

During March 20-23, 2020, it seemed that Saharan dust was transported to southern Sweden as presented in section 4.4. However, during the majority of the time during the afternoon peak event between March 23 and 29, the models did not indicate major import of dust from Sahara, why local or near-regional dust were still the major plausible explanation for this afternoon dust peak event. In the other three afternoon peaks events, there were no signs at all of Saharan dust transport.

In general, it proved to be hard to analyze dust transport from Sahara using ceilometer data. It needs to be investigated closer in the coming if this is a viable method. Maybe it can be combined with other remote sensing LIDAR data from satellites or ground-based

LIDARS?

6.Conclusions

In Hyltemossa, southern Sweden, the identification of natural origin aerosol dust sources, calculation of contribution rates, and identification of transport events were conducted. Observational data from 2018 to 2023 spring seasons were targeted using PM_{10-1} as the variable. Daily average mass concentrations were investigated for occasions with high dust load, and four periods were distinguished based on afternoon dust peaks observed through 1-hour average mass concentrations.

Regarding the afternoon dust peak phenomena in the four periods, the model indicated that three out of four were not caused by Saharan dust transport, but rather were events attributed to dust blowing up from near-regional agriculture or roads, considering the continuous decrease in soil moisture content, rising of the convective boundary layer, and increasing wind speed. No specific trend in wind direction was observed for each period. Sea salt particles showed a strong relationship with wind speed regardless of soil moisture content, but in this study, soil dryness was identified as a common condition causing afternoon dust peaks. However, this condition alone cannot provide conclusive evidence.

The contribution rates of PM_{10-1} during peak times in the four periods were shown to be between 10% and 22%, and the mass concentration of PM_{10-1} during peak times was estimated to be approximately 1 to 2 μg/m^3 as a minimum estimate. Since only peak value contributions were targeted, it is conceivable that the total dust contribution was higher then the minimum estimate. Therefore, it is difficult to accurately calculate the contribution rate of dust based solely on peak contribution rates.

Based on the results of dust models and ceilometer data analysis, it appeared that dust from the Sahara Desert was transported to southern Sweden between March 20 and 23, 2020. However, relying solely on the backscatter of the ceilometer for Saharan dust transport was challenging because distinguishing dust from clouds was not straightforward, and discrimination between dust and other types of particles was not possible. In the future, it is necessary to investigate in detail using other complimentary methods to determine whether this approach is feasible.

7. References

- Basart, S. et al., (2019). *The WMO SDS-WAS Regional Center for Northern Africa, Middle East and Europe.* CADUC 2019
- Carneheim, E.(2020), Planetary boundary layer height measurements in a rural environment in southern Sweden.[Bachelor Thesis, Division of Nuclear Physics, Department of Physics, Lund University]
- EUMET NET, OBSERVATIONS-E-PROFILE, https://www.eumetnet.eu/activities/observations-programme/current-activities/e-profile/. Last accessed March 7, 2024.
- FIDAS manual (2021), *Operating Manual Fine Dust Monitor System*, PALAS GmbH.
- Haby, 2024. https://www.weather.gov/source/zhu/ZHU_Training_Page/clouds/planetary_boundary_layer/PBL.html. Last accessed March 7, 2024.
- ICOS, National Network Sweden, NETWORK AND MESUREMENTS, https://www.icos-sweden.se/node/31. Last accessed March 7, 2024.
- Japan Meteorological Agency https://www.data.jma.go.jp/env/kosahp/kosa_table_titen.html. Last accessed March 15, 2024.
- Kristensson, A.(2005). *Aerosol Particle Sources Affecting the Swedish Air Quality at Urban and Rural Level.* [Doctoral Thesis, Division of Nuclear Physics, Department of Physics, Lund University]
- Malin, G.et al.(2018).*Quantification of population exposure to NO_2, $PM_{2.5}$ and PM_{10} estimated health impacts.* Swedish Environmental Protection Agency.
- Meister, K.et al.(2011).*Estimated Short-Term Effects of Coarse Particles on Daily Mortality in Stockholm, Sweden.* Environmental Health Perspectives, Vol 120, Pages 431-436
- Ministry fo the Environment, Goveranment of Japan https://www.env.go.jp/content/900511203.pdf. Last accessed March 15, 2024
- Ninkovic, S. et al., (2016). *Cloud ice caused by atmospheric mineral dust – Part 1: Parameterization of ice nuclei concentration in the NMME-DREAM model.* European Geosciences Union, Volume16, issue 17, ACP, 16, 11367-11378
- Pérez, C. et al., (2011). *Atmospheric dust modeling from meso to global scales with the online NMMB/BSC-Dust model – Part1: Model description, annual simulations and evaluation.* European Geosciences Union, Volume11, issue 24, ACP, 11, 13001-13027